Jinst

PUBLISHED BY IOP PUBLISHING FOR SISSA

RECEIVED: *October 4, 2010*
ACCEPTED: *November 5, 2010*
PUBLISHED: *November 25, 2010*

Performance of $ZnMoO_4$ crystal as cryogenic scintillating bolometer to search for double beta decay of molybdenum

L. Gironi,[a,b] **C. Arnaboldi,**[a] **J. W. Beeman,**[c] **O. Cremonesi,**[a] **F.A. Danevich,**[d] **V.Ya. Degoda,**[e] **L.I. Ivleva,**[f] **L.L. Nagornaya,**[g] **M. Pavan,**[a,b] **G. Pessina,**[a] **S. Pirro,**[a,1] **V.I. Tretyak**[d] **and I.A. Tupitsyna**[g]

[a] *INFN - Sezione di Milano Bicocca, I 20126 Milano, Italy*
[b] *Dipartimento di Fisica - Università di Milano Bicocca, I 20126 Milano, Italy*
[c] *Lawrence Berkeley National Laboratory, Berkeley, California 94720, U.S.A.*
[d] *Institute for Nuclear Research, MSP 03680 Kyiv, Ukraine*
[e] *Kyiv National Taras Shevchenko University, MSP 03680 Kyiv, Ukraine*
[f] *Institute of General Physics, 119991 Moscow, Russia*
[g] *Institute for Scintillation Materials, 61001 Kharkiv, Ukraine*

E-mail: Stefano.Pirro@mib.infn.it

ABSTRACT: Zinc molybdate ($ZnMoO_4$) single crystals were grown for the first time by the Czochralski method and their luminescence was measured under X-ray excitation in the temperature range 85–400 K. Properties of $ZnMoO_4$ crystal as cryogenic low temperature scintillator were checked for the first time. Radioactive contamination of the $ZnMoO_4$ crystal was estimated as $\leq$ 0.3 mBq/kg (^{228}Th) and 8 mBq/kg (^{226}Ra). Thanks to the simultaneous measurement of the scintillation light and the phonon signal, the α particles can be discriminated from the γ/β interactions, making this compound extremely promising for the search of neutrinoless Double Beta Decay of ^{100}Mo. We also report on the ability to discriminate the α-induced background without the light measurement, thanks to a different shape of the thermal signal that characterizes γ/β and α particle interactions.

KEYWORDS: Cryogenic detectors; Gamma detectors (scintillators, CZT, HPG, HgI etc); Particle identification methods

ARXIV EPRINT: 1010.0103

[1] Corresponding author

doi:10.1088/1748-0221/5/11/P11007

Contents

2010 JINST 5 P11007

1 Introduction

Neutrinoless Double Beta Decay ($0\nu2\beta$) of atomic nuclei is a rare nuclear process able to give very important information about properties of neutrino and weak interaction.

Observations of neutrino oscillations [1–3] give a clear evidence that neutrino is a massive particle. While oscillation experiments are sensitive to the neutrinos squared-mass differences, only the measurement of a $0\nu2\beta$ decay rate could establish the Majorana nature of the neutrino, participate in the determination of the absolute scale of neutrino masses and test lepton number conservation [4–6]. Moreover, this process can clarify the presence of right-handed currents in weak interaction, and prove the existence of Majorons [6]. Taking into account ambiguity of theoretical estimations [7–10], development of experimental methods for different 2β isotopes is highly requested.

^{100}Mo is one of the most promising 2β isotopes because of its large transition energy $Q_{2\beta} = 3035$ keV [11] and a considerable natural isotopic abundance $\delta = 9.67\%$ [12]. From the experimental point of view a large $Q_{2\beta}$ value simplifies the problem of background induced by natural radioactivity and cosmogenic activation.

Nowadays the best sensitivity to $0\nu2\beta$ decay of ^{100}Mo is the one reached by the NEMO experiment [13] that, with $\simeq$7 kg of enriched ^{100}Mo, has obtained a half-life limit $T^{0\nu}_{1/2} > 4.6 \times 10^{23}$ yr at 90% C.L. Despite the beautiful result, the NEMO technique presents two disadvantages that limit the achievable sensitivity: the low detection efficiency of $0\nu2\beta$ events ($\approx 14\%$) and the poor energy resolution ($\approx 10\%$ at the energy of $Q_{2\beta}$ of ^{100}Mo). Both these limitations can be overcome by the use of a high resolution detector containing in its sensitive volume the DBD candidate, i.e. by the use of the so called source=detector technique.[1] In particular, the energy resolution (FWHM $< 1\%$) needed to investigate the normal hierarchy of the neutrino mass (half-life sensitivity on the level of $10^{28} - 10^{30}$ years) could be achieved only by bolometers or/and semiconductors providing an energy resolution of about few keV [16].

[1] For instance the detection efficiency is $\approx 86\%$ in the CUORICINO experiment with 0.75 kg tellurium oxide crystals [14] and $\approx 93\%$ for Ge detectors [15].

Table 1. Properties of $ZnMoO_4$ crystal scintillators.

Density (g/cm^3)	4.3	[31]
Melting point (°C)	1003 ± 5	[31]
Structural type	Triclinic, $P1$	[31, 33]
Cleavage plane	Weak (001)	[31]
Wavelength of emission maximum* (nm)	544	Present work

*Under X-ray excitation at room temperature.

The main issue for the bolometric technique is the suppression -or active rejection- of the background induced by α emitters located close to the surface of a detector. Simulations show that this contribution will largely dominate the expected background of the CUORE Experiment [17, 18] in the region of interest. The natural way to discriminate this background is to use a scintillating bolometer [19]. In such a device the simultaneous and independent read out of the heat and the scintillation light permits to discriminate events due to γ/β, α and neutrons thanks to their different scintillation yield.

Several inorganic scintillators containing molybdenum were developed in the last years. The most promising of them are molybdates of Calcium ($CaMoO_4$) [20, 21], Cadmium ($CdMoO_4$) [19, 22], Lead ($PbMoO_4$) [19, 23, 24], Lithium-Zinc ($Li_2Zn_2(MoO_4)_3$) [25], and Lithium (Li_2MoO_4) [26, 27]. However $CaMoO_4$ contains the $2\nu2\beta$ active isotope ^{48}Ca which, even if present in natural Ca with a very small abundance of $\delta = 0.187\%$ [12], creates background at $Q_{2\beta}$ energy of ^{100}Mo [21]. $CdMoO_4$ contains the β active ^{113}Cd ($T_{1/2} = 8.04 \times 10^{15}$ yr [28], $\delta = 12.22\%$ [12]) which, besides being beta active, has a very high cross section to capture thermal neutrons. A potential disadvantage of $PbMoO_4$ (supposing crystals would be produced from low-radioactive ancient lead [29, 30]) is that ^{100}Mo would be only 27% of the total mass. Finally $Li_2Zn_2(MoO_4)_3$ and Li_2MoO_4 have low Light Yield (LY).

$ZnMoO_4$ crystals were developed only very recently [31, 32]. An important advantage of $ZnMoO_4$ is the absence of heavy elements and high concentration of molybdenum (43% in weight).

The purpose of our work is to investigate $ZnMoO_4$ crystals as scintillating bolometers to search for double beta decay of ^{100}Mo. Luminescence of material was studied under X-ray irradiation. The performances of the detector were measured through the use of the bolometric technique.

2 Growth of $ZnMoO_4$ crystals

The zinc molybdate ($ZnMoO_4$) charge was obtained by a solid-phase synthesis technique from MoO_3 and ZnO powders (both of 99.995% purity). Single crystals of up to dia=30 mm, h=40 mm were grown by the Czochralski technique with a drawing speed of 1.9 mm/h. The material is highly inert; the melting point is at (1003 ± 5) °C. The crystal density calculated from the X-ray data is 4.317 g/cm^3, while the density measured by the pycnometric method is 4.19 g/cm^3 [31]. Properties of $ZnMoO_4$ crystals are presented in table 1.

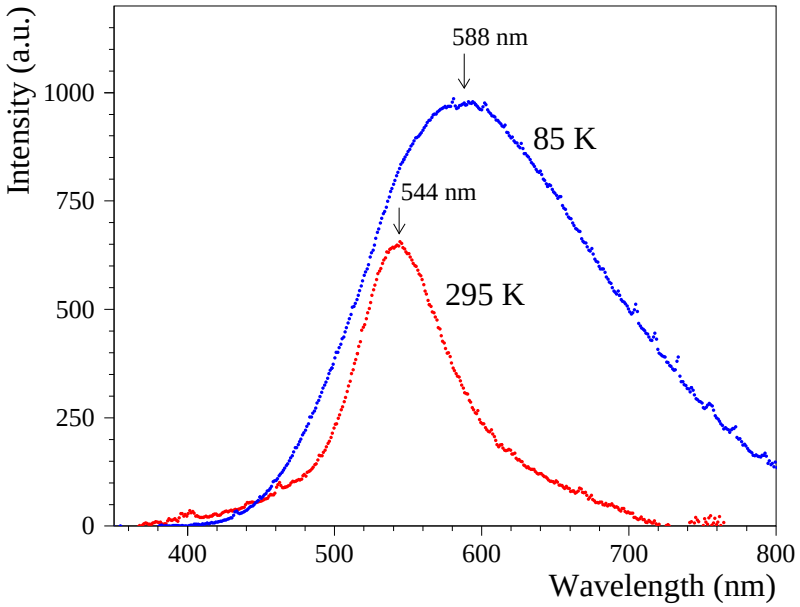

Figure 1. (Color online) Emission spectrum of $ZnMoO_4$ crystal under X-ray excitation at 85 K and 295 K.

3 Luminescence under X-ray excitation

We measured the luminescence of $ZnMoO_4$ crystal in the temperature interval 85–400 K under X-ray excitation. A sample of $ZnMoO_4$ crystal ($10 \times 10 \times 2$ mm^3) was irradiated by X-ray from a BHV7 tube with a rhenium anode (20 kV, 20 mA). The light emitted by the crystal was detected in the visible region by a FEU-106 photomultiplier (sensitive in the wide wavelength region of 300 – 800 nm). Spectral measurements were carried out using a high-aperture MDP-2 monochromator.

One band in the visible region with the maximum at 544 nm was observed at room temperature (figure 1). The radioluminescence (RL) spectrum, measured at 85 K, is shifted to 588 nm. In addition, the spectrum measured at 85 K is much wider and distributed in the wavelength region above 700 nm.

The temperature dependence of luminescence is presented in figure 2. The intensity of luminescence slowly falls above 150 K, but it still remains observable even at $\approx$ 400 K temperature. A sharp peak of thermostimulated luminescence (TSL) was observed at $\approx$ 120 K and across the wide temperature range 220–320 K (see figure 3), with maxima at $\approx$ 230, $\approx$ 260, and $\approx$ 300 K. The TSL observed in our measurements indicates the presence of traps in the $ZnMoO_4$ sample. We assume it is due to defects and impurities in the crystal. Both can deteriorate the scintillation and/or the bolometric performances. Therefore, further R&D is necessary to improve the quality of $ZnMoO_4$ crystals.

4 $ZnMoO_4$ as a scintillating bolometer

We present in this section the results obtained with a small sample (19.8 g) of $ZnMoO_4$ operated as scintillating bolometer. The shape of our sample is a regular hexagon, with a diagonal of 25 mm and a height of 11 mm. The color of the sample is fairly orange, showing evident inclusions along

2010 JINST 5 P11007

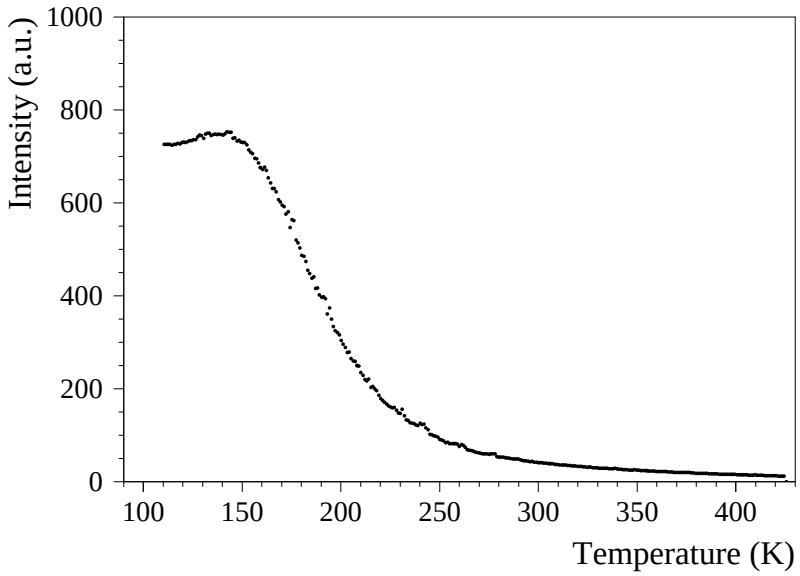

Figure 2. Temperature dependence of $ZnMoO_4$ luminescence intensity under X-ray excitation.

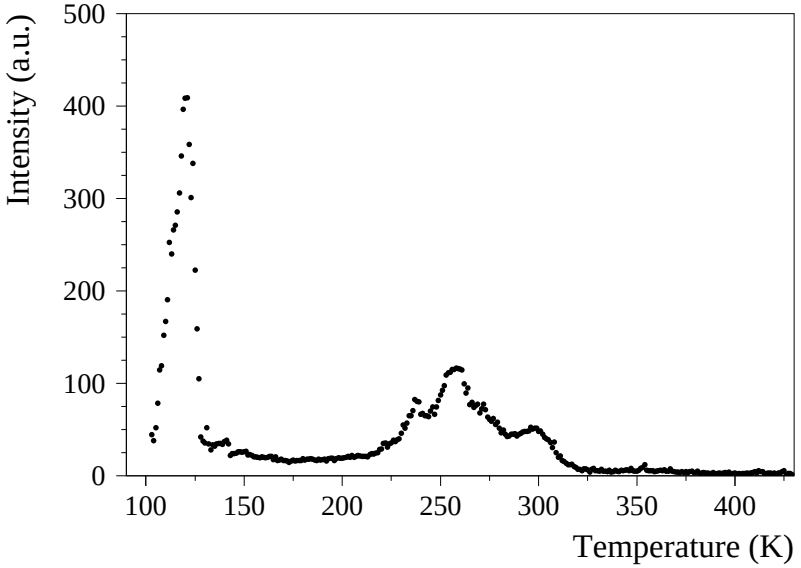

Figure 3. Thermoluminescence of $ZnMoO_4$ crystal after X-ray excitation at liquid nitrogen temperature.

the central axis of the growth. The composite device (bolometer + light detector) is schematized in figure 4. The crystal is held by means of two L-shaped Teflon (PTFE) pieces fixed to two cylindrical Cu frames; the PTFE forces the crystal to the base consisting of a Cu plate covered with an Al foil. The crystal is surrounded by a 25.1 mm diameter cylindrical reflecting foil (3M VM2002). At cryogenic temperatures (10÷100 mK) for which a detector can work as bolometer, no "standard" light detectors can work properly. The best way to overcome this problem is to use a second - very sensitive- "dark" bolometer that absorbs the scintillation light giving rise to a measurable increase of its temperature. Our Light Detector (LD) [34] consists of a 36 mm diameter, 1 mm

2010 JINST 5 P11007

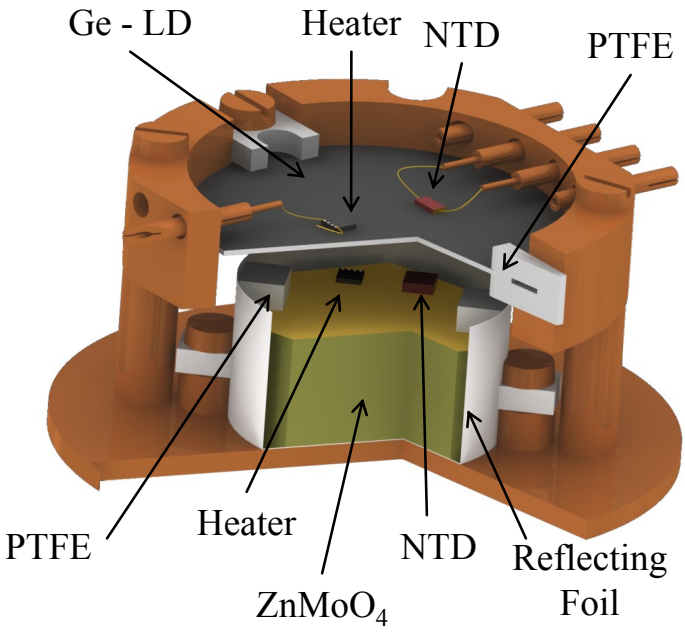

Figure 4. Setup of the detector.

thick pure Ge crystal absorber. The temperature sensor of the $ZnMoO_4$ crystal is a 3x3x1 mm^3 neutron transmutation doped Germanium thermistor, identical to the ones used in the CUORICINO experiment [14]. The temperature sensor of the LD has a smaller volume (3x1.5x0.4 mm^3) in order to decrease its heat capacity, increasing therefore its thermal signal. A resistor of $\sim$300 kΩ, realized with a heavily doped meander on a 3.5 mm^3 silicon chip, is attached to each absorber and acts as a heater to stabilize the gain of the bolometer [35, 36]. The detectors were operated deep underground in the Gran Sasso National Laboratories in the CUORE R&D test cryostat. The details of the electronics and the cryogenic facility can be found elsewhere [37–39].

The heat and light pulses, produced by a particle interacting in the $ZnMoO_4$ crystal and transduced in a voltage pulse by the NTD thermistors, are amplified and fed into a 16 bit NI 6225 USB ADC unit. The entire waveform (*raw pulse*) of each triggered voltage pulse is sampled and acquired. The amplitude V^{heat} and the shape of the voltage pulse is then determined by the off-line analysis that makes use of the Optimal Filter (OF) technique [17, 40]. The signal amplitudes are computed as the maximum of the optimally filtered pulse, while the signal shape is evaluated on the basis of four different parameters: τ_{rise} and τ_{decay}, TVL and TVR.

τ_{rise} (the rise time) and τ_{decay} (the decay time) are evaluated on the *raw pulse* as ($t_{90\%}$-$t_{10\%}$) and ($t_{30\%}$-$t_{90\%}$) respectively. The rise time is dominated by the time constant of the absorber-glue-sensor interface (as well as the heat capacity), while the decay time is determined by the crystal heat capacity and by its thermal conductance toward the heat sink.

TVR (Test Value Right) and TVL (Test Value Left) are computed on the optimally filtered pulse as the least square differences with respect to the filtered response function[2] of the detector:

[2]The response function of the detector, i.e. the shape of a pulse in absence of noise, is computed with a proper average over a large number of raw pulses. It is also used, together with the measured noise power spectrum, to construct the transfer function of the Optimal Filter.

2010 JINST 5 P11007

Table 2. Main parameters of the $ZnMoO_4$ bolometer and light detector. The OF (Optimum Filter) FWHM represent the theoretical energy resolution as evaluated from the signal-to-noise ratio. The (absolute) Signal represents the voltage read across the thermistor for a unitary deposition of energy.

	Resistance [MΩ]	OF FWHM [keV]	τ_{rise} [ms]	τ_{decay} [ms]	Signal [μV/MeV]
$ZnMoO_4$	2.5	1.6	12.2	59.5	107
LD	14.5	0.48	4.0	14.3	1490

TVR on the right side of the optimally filtered pulse maximum and TVL on the left. In fact TVR measures the shape difference of each sampled pulse with respect to the "average thermal pulse" (i.e. the response function), evaluating this difference within the "falling side" of the pulse. TVL makes use of the same algorithm, but is evaluated on the "rising side" of the pulse. These two parameters do not have a direct physical meaning, however they are extremely sensitive (even in noisy conditions) to any difference between the shape of the analyzed pulse and the response function. Consequently, they are used either to reject fake triggered signals or to identify variations in the pulse shape with respect to the response function (and this will be our case).

The thermal pulses are acquired within a 512 ms time window with a sampling rate of 2 kHz. The trigger of the $ZnMoO_4$ is software generated while the LD is automatically acquired in coincidence with the former.

The energy calibration of the $ZnMoO_4$ crystal is performed using γ sources (^{232}Th) placed outside the cryostat. The energy calibration of the LD, on the contrary, is obtained thanks to a weak ^{55}Fe source placed close to the Ge that illuminates homogeneously the face opposed to the $ZnMoO_4$ crystal. During the LD calibration its trigger is set independent from the one of the $ZnMoO_4$. The LD is calibrated using a simple linear function. The main parameters of the two bolometers are listed in table 2.

Two sets of data have been collected with this device: a calibration using external ^{232}Th sources (65 h) and a background measurement (66 h). The temperature of the detectors during our test was $\sim$ 14 mK. The intensity of the calibration sources was not optimized for small crystals, so that the statistics collected within the calibration peaks of $ZnMoO_4$ is rather poor. The energy resolution evaluated at 911, 2615 and at 5407 keV (^{228}Ac, ^{208}Tl and internal contamination of ^{210}Po, respectively) are 3.6$\pm$1, 5.6$\pm$2 and 6$\pm$1 keV, respectively. The FWHM energy resolution of the LD, evaluated on the X doublet at 5.90 and 6.49 keV, is 470$\pm$20 eV.

In this field the usual way to present the results is to draw the light vs. heat scatter plot [41]. Here each event is identified by a point with abscissa equal to the heat signal (recorded by the $ZnMoO_4$ bolometer), and ordinate equal to the light signal (simultaneously recorded by the LD). In the scatter plot, γ/β and α give rise to separate bands, in virtue of their characteristic light to heat ratio. In figure 5 we present the scatter plot light vs. heat of the sum of the two above mentioned measurements (Calibration + Background). The LY of this crystal (measured on the 2615 keV ^{208}Tl line) can be evaluated as 1.1 keV/MeV. This value is rather small. Using the same LD we evaluated the LY of a large (510 g) $CdWO_4$ crystal to be 17.4 keV/MeV [41]. Nonetheless it is evident from

2010 JINST 5 P11007

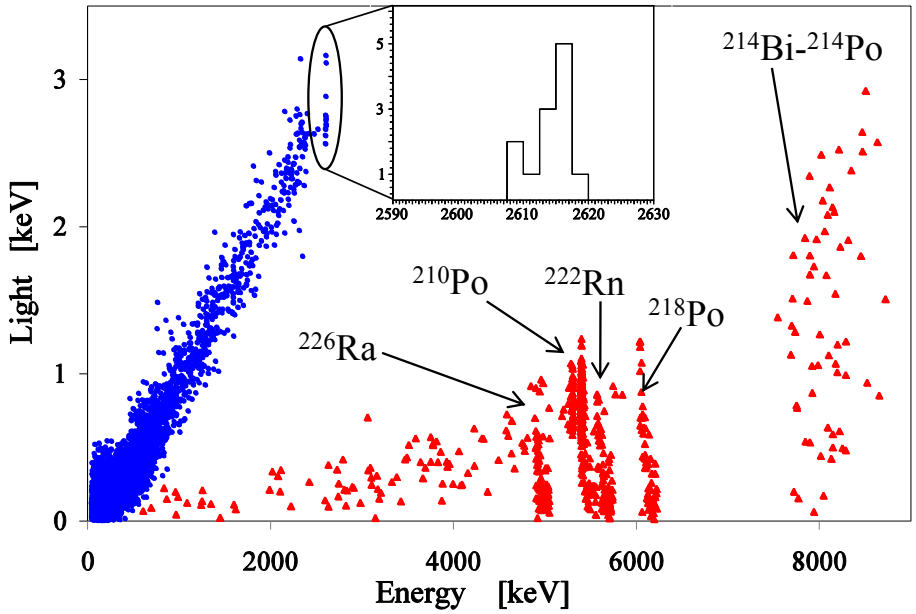

Figure 5. Scatter plot light vs. heat obtained with a ^{232}Th calibration (65 h) plus a background measurement (66 h). The main observed lines are pointed out. In the inset the 2615 keV γ-line of ^{208}Tl. The dark (blue) points are identified as γ/β events, while the light (red) triangles are identified as α-particles. The BiPo points are due to mixed events induced by a γ/β decay "immediately" followed by an α decay, with τ=164 μs, too fast for both our detectors to be distinguished from the parent γ/β.

figure 5 that the continuous background induced by α-emitters located close to the surfaces is very efficiently recognized with respect to the γ/β events. The γ/β band is mainly due to the interaction of γ rays produced from the calibration source or from radioactive contamination of the detector and its set-up. The events in the α band are due to intrinsic radioactive contamination of ^{226}Ra, of the ^{238}U chain. The continuum below the ^{226}Ra peak can be ascribed to an alpha contamination in the surfaces of the mounting structure, producing degraded alpha particles with a continuous distribution of energies. ^{214}Bi-^{214}Po events are due to the fast decay chain of these two isotopes that produce a beta followed by an alpha, with a time separation below the integration time of the detector (i.e. they are recorded as a single event with an energy corresponding to the sum of α and β energies).

A strange feature has however to be pointed out: all the α-lines are characterized by a tail that draws negative slopes "bands", as it is apparent in figure 5. This effect is extremely evident in the α-peaks induced by ^{226}Ra, ^{222}Rn and ^{218}Po. This results in a large smearing of the energy resolution of these peaks. The "doublet" due to ^{210}Po, instead, shows this unexpected feature only -very marginally- on the full energy peak, at 5407 keV line.

This strange behavior is likely when the contaminations are close to the surfaces, both of the crystal and of the surrounding materials. The presence of large quantity of surface contaminants, in fact, is corroborated by the large α-continuum background, visible in the same figure. This issue should be studied in more details. This is however beyond the scope of this work. Moreover this effect — even if not well understood — increases the separation between α and γ/β interactions

2010 JINST 5 P11007

Table 3. Radioactive α activity of $ZnMoO_4$ crystal. The activity in ^{232}Th corresponds to a limit in the contamination of $7{\cdot}10^{-11}$ g/g. The contamination in ^{238}U has a limit of $2{\cdot}10^{-11}$ g/g. The observed ^{226}Ra contamination, instead, would correspond — assuming secular equilibrium — to a contamination of ^{238}U = $6{\cdot}10^{-10}$ g/g.

Chain	Nuclide	Activity (mBq/kg)
^{232}Th	^{232}Th	≤ 0.3
	^{228}Th	≤ 0.3
^{238}U	^{238}U	≤ 0.2
	^{234}U	≤ 0.8
	^{230}Th	≤ 0.3
	^{226}Ra	8.1 ± 0.3
	^{210}Po	28 ± 2
Total α activity		73 ± 2

in the scatter plot. Nonetheless, by assuming, in a very conservative way, that all the observed α lines are induced by internal contamination, we obtained the values in table 3.

It can be seen that, as it very often happens, the ^{238}U chain is broken at ^{226}Ra. With respect to the ^{232}Th decay chain, the most dangerous [19] internal contaminant for this kind of detectors, we only observe a limit.

A very interesting feature of this compound comes from the observation that α and γ/β events give rise to slightly different thermal pulses. In fact this promising feature was very recently exploited in $CaMoO_4$ [42] as well as, even if less pronounced, in ZnSe [43].

In figure 6 we show the Pulse Shape Analysis performed only on the heat signal read in the $ZnMoO_4$ crystal. The separation between α and γ/β events is rather impressive, especially in the left panel of figure 6. A comparison of the two distributions in the 2400–2620 keV energy region shows a separation of 7.2 σ. This result needs further investigation with a high statistics comparison in the 3 MeV energy region (the $Q_{2\beta}$ value of ^{100}Mo). It expresses however in a quantitative way the excellent rejection power of this technique.

5 Conclusions

Zinc molybdate ($ZnMoO_4$) single crystals were grown for the first time by the Czochralski method. Luminescence was measured under X-ray excitation in the temperature range 85–400 K. Emission maximum of $ZnMoO_4$ occurs at 544 nm at 295 K, and then shifts to 588 nm at 85 K.

Applicability of $ZnMoO_4$ crystals as cryogenic phonon-scintillation detectors was demonstrated for the first time. Despite the "non perfect" quality of our crystal sample, we obtained very encouraging results. The light output of $ZnMoO_4$ was estimated $< 6\%$ comparatively to $CdWO_4$. Even if rather small, the scintillation signal permits a very efficient discrimination between α and γ/β particles.

Especially this compound shows a different heat pulse shape between α and γ/β events. This permits the discrimination of the α induced background -*without* using the scintillation signal-

2010 JINST 5 P11007

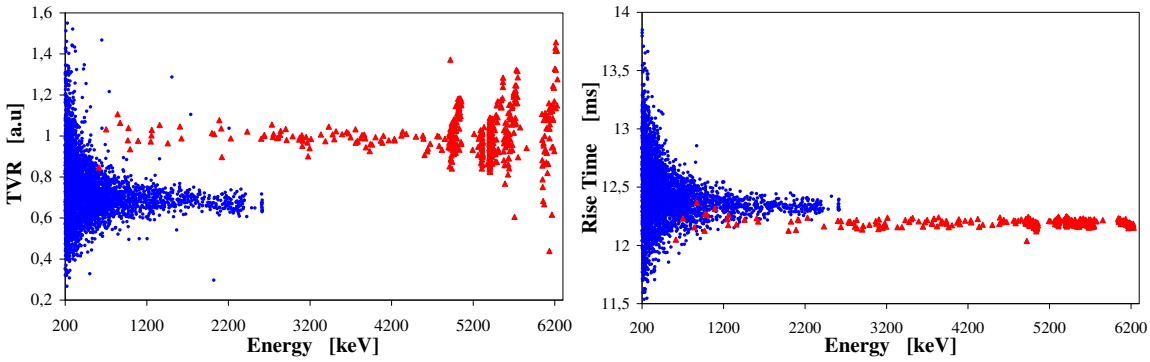

Figure 6. Pulse Shape Analysis of the events of figure 5. Left panel: TVR of the heat signal in $ZnMoO_4$ vs. energy (heat). The α events are effectively discriminated with respect to γ/β events down to low energies. Right panel: τ_{rise} of heat pulses vs. energy (heat) for the same events. It has to be pointed out, however, that the two parameters (τ_{rise} and TVR) are largely uncorrelated since one is calculated on the left part of the pulse maximum, while the latter on the right. Thus their combination will further increase the discrimination factor.

at a level of 7.2 σ. This feature could play a crucial role for a possible large scale double beta decay experiment.

Acknowledgments

The results reported here have been obtained in the framework of the Bolux R&D Experiment funded by INFN, aiming at the optimization of a cryogenic DBD Experiment for a next generation experiment. Thanks are due to E. Tatananni, A. Rotilio, A. Corsi and B. Romualdi for continuous and constructive help in the overall setup construction. Finally, we are especially grateful to Maurizio Perego for his invaluable help in the development and improvement of the Data Acquisition software. The work of F.A. Danevich and V.I. Tretyak was partially supported by the Project "Kosmomikrofizyka-2" (Astroparticle physics) of the National Academy of Sciences of Ukraine.

References

[1] R.N. Mohapatra et al., *Theory of neutrinos: a white paper*, *Rep. Prog. Phys.* **70** (2007) 1757 [hep-ph/0510213v2].

[2] G.L. Fogli et al., *Observables sensitive to absolute neutrino masses: A reappraisal after WMAP 3-year and first MINOS results*, *Phys. Rev.* **D 75** (2007) 053001 [hep-ph/0608060].

[3] G.L. Fogli et al., *Observables sensitive to absolute neutrino masses. II* *Phys. Rev.* **D 78** (2008) 033010 [arXiv:0805.2517].

[4] A. Strumia and F. Vissani, *Neutrino masses and mixings and...*, (2010) hep-ph/0606054v3.

[5] S.R. Elliott and J. Engel, *Double Beta Decay J. Phys.* **G 30** (2004) 183 [hep-ph/0405078v2].

[6] F.T. Avignone III, S.R. Elliott and J. Engel, *Double beta decay, Majorana neutrinos, and neutrino mass*, *Rev. Mod. Phys.* **80** (2008) 481.

[7] F. Simkovic et al., *Anatomy of nuclear matrix elements for neutrinoless double-beta decay*, *Phys. Rev.* **C 77** (2008) 045503 [arXiv:0710.2055].

2010 JINST 5 P11007

[8] O. Civitarese and J. Suhonen, *Nuclear matrix elements for double beta decay in the QRPA approach: A critical review*, *J. Phys. Conf. Ser.* **173** (2009) 012012.

[9] J. Menendez, et al., *Disassembling the Nuclear Matrix Elements of the Neutrinoless double beta Decay*, *Nucl. Phys.* **A 818** (2009) 139 [arXiv:0801.3760].

[10] J. Barea and F. Iachello, *Neutrinoless double-beta decay in the microscopic interacting boson model*, *Phys. Rev.* **C 79** (2009) 044301.

[11] G. Audi, A.H. Wapstra, C. Thibault, *The AME 2003 atomic mass evaluation: (II). Tables, graphs and references*, *Nucl. Phys.* **A 729** (2003) 337.

[12] J.K. Bohlke et al., *Isotopic Compositions of the Elements, 2001*, *J. Phys. Chem. Ref. Data* **34** (2005) 57.

[13] R. Arnold et al., *First Results of the Search for Neutrinoless Double-Beta Decay with the NEMO 3 Detector*, *Phys. Rev. Lett.* **95** (2005) 182302.

[14] C. Arnaboldi et al., *Results from a search for the 0-neutrino-decay of 130-Te*, *Phys. Rev.* **C 78** (2008) 035502.

[15] H. Gomez et al., *Background reduction and sensitivity for germanium double beta decay experiments*, *Astropart. Phys.* **28** (2007) 435 arXiv:0708.3987.

[16] Yu.G. Zdesenko, F.A. Danevich, V.I. Tretyak, *Sensitivity and discovery potential of the future 2beta decay experiments*, *J. Phys.* **G 30** (2004) 971.

[17] C. Arnaboldi et al., *CUORE: a cryogenic underground observatory for rare events*, *Nucl. Instrum. Meth.* **A 518** (2004) 775.

[18] M. Pavan et al., *Control of bulk and surface radioactivity in bolometric searches for double-beta decay*, *Eur. Phys. J* **A 36** (2008) 159.

[19] S. Pirro et.al, *Scintillating double-beta-decay bolometers*, *Phys. Atom. Nucl.* **69** (2006) 2109 [nucl-ex/0510074].

[20] S. Belogurov et al., *CaMoO4 Scintillation Crystal for the Search of 100-Mo Double Beta Decay*, *IEEE Trans. Nucl. Sci.* **52** (2005) 1131.

[21] A.N. Annenkov et al., *Development of CaMoO4 crystal scintillators for a double beta decay experiment with 100-Mo*, *Nucl. Instrum. Meth.* **A 584** (2008) 334.

[22] V.B. Mikhailik and H. Kraus, *Cryogenic scintillators in searches for extremely rare events*, *J. Phys.* **D 39** (2006) 1181.

[23] F.A. Danevich et al., *Feasibility study of PbWO4 and PbMoO4 crystal scintillators for cryogenic rare events experiments*, *Nucl. Instrum. Meth.* **A 622** (2010) 608.

[24] M. Minowa et al., *Measurement of the property of cooled lead molybdate as a scintillator*, *Nucl. Instrum. Meth.* **A 320** (1992) 500.

[25] N.V. Bashmakova et al., *$Li_2Zn_2(MoO_4)_3$ crystal as a potential detector for ^{130}Mo 2β-decay search*, *Funct. Mater.* **16** (2009) 266.

[26] O.P. Barinova et al., *Intrinsic radiopurity of a Li2MoO4 crystal* *Nucl. Instrum. Meth.* **A 607** (2009) 573.

[27] O.P. Barinova et al., *First test of Li2MoO4 crystal as a cryogenic scintillating bolometer*, *Nucl. Instrum. Meth.* **A 613** (2010) 54.

[28] P. Belli et al., *Investigation of beta decay of 113Cd*, *Phys. Rev.* **C 76** (2007) 064603.

2010 JINST 5 P11007

[29] A. Alessandrello et al., *Measurements of internal radioactive contamination in samples of Roman lead to be used in experiments on rare events*, *Nucl. Instr. and Meth.* **B 142** (1998) 163.

[30] F.A. Danevich et al., *Ancient Greek lead findings in Ukraine*, *Nucl. Instrum. Meth.* **A 603** (2009) 328.

[31] L.I. Ivleva et al., *Growth and properties of ZnMoO4 single crystals*, *Crystal. Rep.* **53** (2008) 1087.

[32] L.L. Nagornaya et al., *Tungstate and Molybdate Scintillators to Search for Dark Matter and Double Beta Decay* *IEEE Trans. Nucl. Sci.* **56** (2009) 2513.

[33] W. Reichelt et al., *Mischkristallbildung im System CuMoO4/ZnMoO4*, *Zeit. Anorg. Allg. Chemie* **626** (2000) 2020.

[34] S. Pirro et al., *Development of bolometric light detectors for double beta decay searches*, *Nucl. Instrum. Meth.* **A 559** (2006) 361.

[35] A. Alessandrello et al., *Methods for response stabilization in bolometers for rare decays*, *Nucl. Instrum. Meth.* **A 412** (1998) 454.

[36] C. Arnaboldi, G. Pessina and E. Previtali, *A programmable calibrating pulse generator with multi-outputs and very high stability*, *IEEE Tran. Nucl. Sci.* **50** (2003) 979.

[37] S. Pirro, *Further developments in mechanical decoupling of large thermal detectors*, *Nucl. Instrum. Meth.* **A 559** (2006) 672.

[38] C. Arnaboldi, G. Pessina and S. Pirro, *The cold preamplifier set-up of CUORICINO: Towards 1000 channels*, *Nucl. Instrum. Meth.* **A 559** (2006) 826.

[39] C. Arnaboldi et al., *The front-end readout for CUORICINO, an array of macro-bolometers and MIBETA, an array of micro-bolometers*, *Nucl. Instrum. Meth.* **A 520** (2004) 578.

[40] E. Gatti and P.F. Manfredi, *Processing the signals from solid-state detectors in elementary-particle physics*, *Riv. Nuovo Cim.* **9** (1986) 1.

[41] C. Arnaboldi et al., *CdWO4 scintillating bolometer for Double Beta Decay: Light and heat anticorrelation, light yield and quenching factors*, *Astrop. Phys.* **34** (2010) 143 [arXiv:1005.1239].

[42] L. Gironi, *Scintillating bolometers for Double Beta Decay search*, *Nucl. Instrum. Meth.* **A 617** (2010) 478.

[43] C. Arnaboldi et al., *Characterization of ZnSe scintillating bolometers for Double Beta Decay*, accepted by Astropart. Phys. [arXiv:1006.2721v2].

2010 JINST 5 P11007